International Journal of
INTELLIGENT SYSTEMS AND APPLICATIONS IN ENGINEERING
ISSN:2147-6799 www.ijisae.org Original Research Paper

AI-Based Anti-Islanding Protection Algorithm for Grid Tied PV System

Aashish Jaiswal[1], Dr. Subhash Chandra[2], Dr. Sulabh Sachan[3]

Submitted: 04/02/2024 **Revised**: 12/03/2024 **Accepted**: 18/03/2024

Abstract: This study presents novel strategies for recognizing islanding and shows what it means for Matrix Associated Photovoltaic (PV) Exhibits. One normal sort of DG that is many times put in frameworks that are connected to the lattice is photovoltaic (PV). By the by, network associated frameworks keep on confronting the significant test of inadvertent islanding. To upgrade PV lattice associated innovation, an enemy of islanding identifying regulator is frequently used to stay away from coincidental islanding. This study presents an examination of dynamic and latent enemy of islanding recognition draws near. Dynamic Recurrence Float (AFD) and Voltage and recurrence Assurance (OVP/UVP and OFP/UFP) are two inactive and dynamic enemy of islanding identification strategies, separately, and their ideas are portrayed. The investigated enemy of islanding methods are mimicked in this paper utilizing the MATLAB/Simulink programming. While the recreation results show that the dynamic methodology further develops the power nature of the framework, the uninvolved system, sadly, has non-recognition zones. In a lattice tied PV framework, this study tries to give an overall information on enemy of islanding strategies upheld by simulated intelligence.

Keywords: *frameworks, PV, islanding, simulated, strategies, portrayed*

I. Introduction

At the point when a part of the utility framework's electrical cable — including DERs and burdens — is separated from the fundamental power network yet remains zapped, this peculiarity is known as islanding or loss of matrix/principal (LOG/LOM). Moreover, "islanding" portrays a situation where DER are enacted beyond the Purpose In like manner Coupling (PCC) while simultaneously electrically confining one area of the Electric Power Framework (EPS) from the other EPS [1]. The reasons for islanding may be either conscious or inadvertent.

An arranged islanding is one that has been painstakingly thought of, while an impromptu one has been taken a risk with. The accidental structure is the most hazardous since it relies upon the inadvertent exhaustion of some EPS while the DER power is still there, as opposed to the equilibrium of the EPS. To advance DER reconciliation into the power framework without DER shortcomings, further developing dependable and exact enemy of islanding solutions is basic. Subsequently, ensuring all Enemy of Islanding (simulated intelligence) prerequisites are considered is the genuine test while fostering a sun based inverter [2]. One of the trickiest parts is distinguishing islanding in a receptive style, which leaves the entire framework open to startling errors. At the point when the fundamental power is switched off out of the blue, yet the PV inverter stays associated and keeps running with a heap, this is called islanding in photovoltaic power frameworks, which are a kind of disseminated energy asset [3].

It is much of the time to the point of utilizing a blend of under/over voltage/recurrence security to stay away from islanding, yet generally speaking it is important to promptly detach the PV framework from the power lattice upon recognition of islanding. To improve PV matrix associated frameworks, this study presents a near examination of hostile to islanding identification calculations [4]. Detached and dynamic techniques for recognizing islands are likewise shrouded in the review. The last method of recognition is dynamic recurrence float (AFD), while the previous methodologies are under voltage and over voltage assurance (UVP/OVP) and under recurrence and over recurrence security (UFP/OFP). The investigated enemy of islanding strategies are reproduced in this paper utilizing the MATLAB/Simulink programming. After this, we will wrap up our conversation and investigation of the reenactment discoveries.

II. Literature Review

The most common way of making an island state is known as island creation. There are two particular kinds of island arrangement, one related with issues and the other with upkeep.

Islanding happens when the essential dispersion framework encounters a disappointment. Envision a short blackout when the circulated generator (DG) was turned off from the fundamental framework and thusly associated with the significant burden, bringing about an

[1]*Scholar, Department of Electrical Engineering, GLA University, Mathura*
[2]*Guide- Associate Professor, GLA University Mathura*
[3]*Co Guide- Assistant Professor, GLA University Mathura*
[1]*Email: aashish.jaiswal@gla.ac.in*
[2]*Email: subhash.chnadra@gla.ac.in*
[3]*Email: sulabh.sachan@gla.ac.in*

island impact of around 20 centimeters. The most concerning issue in setting up the island is the limit hole between the interest for load and the stockpile of DG. The DG limit is the complete weight, an island could create, and it happens very sometimes. The generator's security include was enacted in light of the fact that there was a huge recurrence contrast, despite the fact that the complete adjusted load was logical inside the recurrence scope of the DG source. During the hazardous condition, it is expected that the breaking down part isn't getting power since it is disengaged from the principal network. Along these lines, the soundness of the power matrix is compromised. Portions of the fundamental framework are disconnected in the event of islanding for inspectional checking. This work gives a succinct outline of faltering's experience and the most recent discoveries on scientific and mathematical techniques for recurrence examination [5].

III. Methods For Islanding Detection

As indicated by the IEEE standard for framework interconnection (1547), DGs that are connected to the lattice earn an essential college education of security through the under/over voltage and recurrence insurance (UFP/OFP and UVP/OVP) strategies. For its minimal expense, simplicity of utilization in limited scope frameworks, and quick enemy of islanding recognition time, Dynamic Stage Float (AFD) was chosen as the dynamic technique [6]. A careful examination of the dynamic and detached islanding discovery methods is introduced in the segments that follow.

- **Method for detecting passive islanding: Voltage and Frequency Protection**

Standard wellbeing transfers or voltage irregularity identifiers go by one or two names: UFP/OFP and UVP/OVP. This strategy is fundamental for all matrix associated planetary groups since it gives a key insurance to them. The reason for this is to guarantee that the DG will slice capacity to the utility if the PCC voltage abundancy (Vpcc) or recurrence (Fpcc) goes over as far as possible [7]. Accordingly, the OFP/UFP and OVP/UVP strategies guard against islands, yet additionally distinguish them.

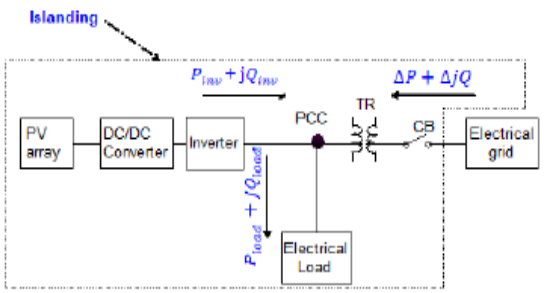

Fig.1.Model of a grid-disconnected DG source (islanding phenomenon)

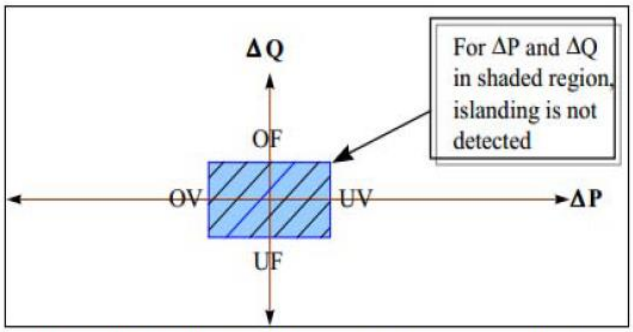

Fig. 2. NDZ in P versus Q for over/ under frequency and voltage.

In Figure 1, we can see the power stream and Purpose In like manner Coupling (PCC) of a nearby planet group that is connected to the lattice.

The PCC goes about as a hindrance between the utility framework and the PV DG's Power Molding Unit (PCU) [8]. The utility associated with the PV framework is shut while running in standard mode. At the point when the power network is cut off, the PV framework's dynamic power yield (Ppv) isn't equivalent to the dynamic power interest (Pload) of the nearby burden. Vpcc should go up or down since the qualities depend on it until Ppv= Pload. Likewise, if the responsive power prerequisites of the neighborhood load (Qload) and the receptive power generator (Qpv) are inconsistent, there will be a network disengage. To get Qpv=Qload, you need to change the Fpvv. The photovoltaic inverter will search for a recurrence at which the stage point between the PV framework and the nearby burden's momentum voltage is equivalent.

Consequently, voltage and recurrence varieties might be recognized by the UVP/OVP and UFP/OFP transfers [9].

It is challenging to distinguish islanding when the PV producing is shut and the neighborhood load request is high since the power variance values are moderate. For NDZ, there isn't sufficient dynamic power variety (ŔQ), in this manner the UFP/OFP and UVP/OVP transfers can't recognize voltage or recurrence changes simultaneously. Since the OVP/UVP security isn't stumbling the utility for this situation, islanding may in any case happen [10].

$$\left(\frac{V}{V_{max}}\right)^2 - 1 \le \frac{\Delta P}{P} \le \left(\frac{V}{V_{min}}\right)^2 - 1 \qquad (1)$$

$$1 - \left(\frac{f}{f_{min}}\right)^2 \le \frac{\Delta Q}{P} \le 1 - \left(\frac{f}{f_{max}}\right)^2 \qquad (2)$$

You can address the association between power confound, voltage, and recurrence utilizing Conditions (1) and (2). Fig. 2 shows the NDZ for 88%-every available ounce of effort of PCC (Vrms) and 98.83%-100.83% of PCC not

entirely settled by Eqs (1) and (2). Contingent upon the cutoff points set for voltage and recurrence, lattice association and islanding might be depicted in an unexpected way. Be extremely mindful so as to separate islanding from other framework interferences while settling on the limit levels. Picture 2 For rms, the NDZ vacillates somewhere in the range of 98.83% and 100.83%, while for rms, it fluctuates from 88% to 110%.When the nearby burden and PV power are practically equivalent, critical to create islanding arrangements can deal with the situation. A close to zero NDZ is the objective of all islanding location techniques.

• Method for detecting active islanding: AFD

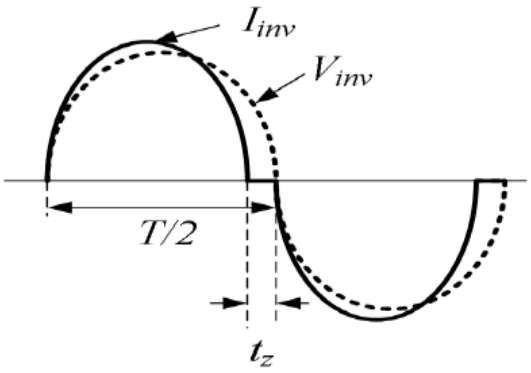

Fig.3.waveform of AFD Technique.

For the AFD technique to work, PCC should be utilized to infuse matrix current with a predisposition signal that is fairly higher in recurrence than network voltage. Utilizing positive criticism, this strategy — otherwise called recurrence inclination — marginally skews the stage point of the inverter's result current. Yet, the power factor resets itself each half cycle and stays nearer to the utility matrix, as displayed in Figure 3 [11].

$$C_f = \frac{2t_z}{T} \qquad (3)$$

As found in Condition (3), the hacking division (Cf) is characterized. The ongoing result from the PV inverter is portrayed by a sinusoid in the main portion of the cycle, with a recurrence that is to some degree more noteworthy than the utility voltage. Upon the PV inverter's result current arriving at nothing, the second period of the cycle starts. During that time, it stays at nothing. Toward the beginning of the final part cycle, the current being delivered by the PV inverter is equivalent to the negative portion of the sine wave from the primary half-cycle. In the wake of getting back to nothing, the ongoing moving through the PV inverter stays at that level until the utility voltage arrives at the zero intersection again [12]. Recall that the last part of the cycle makes some zero memories that isn't equivalent nor fixed; this is vital.

Since the utility network gives a steady stage and recurrence reference, which balances out the Vpcc, the Cf is low when the matrix is associated. At the point when the power framework is removed, a stage confuse shows up in the ɜ and waveforms. At the point when the recurrence is expanded by the PV inverter, the stage blunder is taken out. Once more, the no intersection of the heap voltage reaction pushes ahead in time comparable to its arranged position, and the PV inverter continues to find stage blames and builds its recurrence [17]. On account of this repetitive cycle, the ipv-inv recurrence rises step by step until it varies enough from W0 to be recognized by the OFP/UFP. Upon recognition, it will start the inverter's closure method.

IV. Results And Discussion

- **VFP simulation and outcome**

The commonplace working voltage at the PCC was utilized to create the reenactment, per IEEE standard 1547. The power change coefficient (PCC) recurrence is somewhere in the range of 98.83% and 100.83% of the lattice recurrence, while the matrix voltage is somewhere in the range of 88% and every available ounce of effort at the PCC [13]. At 240 V and 50 Hz, the matrix supply can't distinguish islanding. The working window is 211 V - 264 V on a 240 V base, subsequently the voltage security stumbling point will be set at 210 V and 265 V, separately. If you have any desire to ensure the recurrence trip include is working, you ought to really look at it at 49.3 Hz and 50.5 Hz, individually.

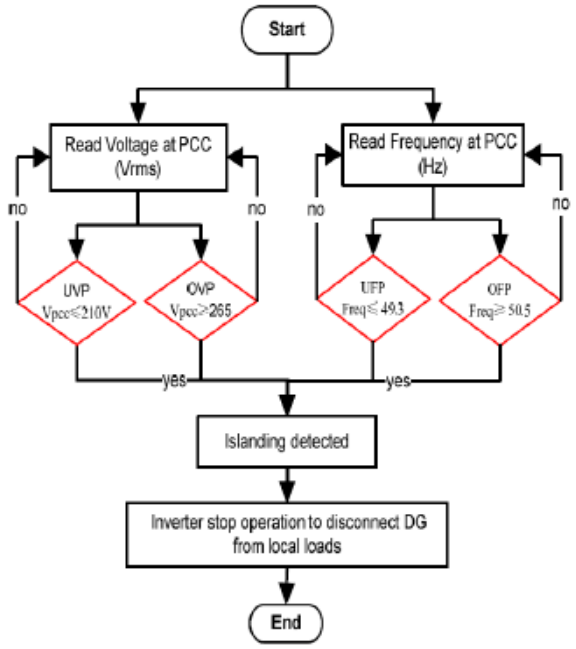

Figure 4: VFP operating flow chart

Here is the VFP functional stream diagram, as displayed in Figure 4. At the PCC, where the lattice disengagement was set at t=0.5 s, a recreation model was utilized to look

at the recurrence and root mean square voltage (Vrms). Consequently, it is vital for the clearing time for UFP/OFP recognition to be under 0.62 seconds and the time it takes to recognize UVP/OVP to be under 2.9 seconds.

Moreover, the consequences of the recreation show that the time it takes to recognize islanding increments for atypical frequencies with values near the limit [14].

The VFP, then again, misses the islanding when an enormous NDZ falls inside the limit. Under ordinary working conditions, the reenacted yield waveforms are displayed in Figures 5 and 6 [see appendix].

Figures 7 and 8 show the underfrequency case's result waveforms (see informative supplement), while Figures 9 and 10 show the overfrequency case's outcomes (see addendum).

- **Simulation and outcome: Drift in Active Frequency**

An earlier hypothetical clarification utilizing AFD is utilized to fabricate a 1 kW single-stage sun oriented power producing framework in Matlab/Simulink. The Vpcc and [16] were to be checked by this control. The control will educate the inverter to slice capacity to the neighborhood load on the off chance that the voltage and recurrence go over the limits set by IEEE 1547. The reproduction module integrates the inverter circuit that is associated with the utility matrix control and the AFD islanding location part of the PCC. To foster the abilities of the AFD regulator module, Matlab/Simulink's s-capability was utilized. The VPCC and are in stage at the primary arrangement. To figure out the PV yield, we changed the matrix supply to 155/50 Hz and the DC voltage to 400 V. L=6 mH and R=0.01 are the RL channels' comparing values. In the first place, at 49.3 Hz, and afterward at 50.5 Hz, was the recurrence assurance limit set. Set at 2.5, the RLC load boundaries were as per the following: R=6.06, L=7.65 mH, and C=1300 uF. The arranged end of the lattice supply happened at t=0.1 s.

Hence, the means of the AFD identification calculation Social event recurrence information and contrasting it with the UFP/OFP standards was the most important phase in deciding if islanding had happened or not [18]. At half-cycle spans (or once per cycle without a trace of islanding) the inverter infuses a recurrence changed source into the result current waveform. The worth of π will rise to some degree each half cycle to move the ongoing recurrence away from the voltage recurrence until islanding is recognized and a sign is shipped off prevent the inverter from working.

IV Conclusion

In this review, two methodologies for distinguishing islands were examined: dynamic identification (AFD) and

Alluding to the reference section, Figures 11-13 demonstrate the models for the AFD regulator; in the NTZ, the VFP neglected to recognize these occasions. Fig. 11 shows the AFD recreation result for the given example πρƒπ=49.4 Hz, =0.049, with a discovery season of t=0.1006 s and πɔ reaching a stand-still at t=0.1594 s, displaying an all out consonant mutilation (THD) of 2.23%. Fig. 12 shows what is going on where πρπF=50.0 Hz, =0.05, the discovery time t=0.1591 s, and the heap ππρπF totally stops at t=0.2171 s with an all out consonant contortion (THD) of 3.91%. In Figure 13, we can notice a model where ππρ=50.4, =0.0504, t=0.1005 s, and a stand-still at t=0.0.1672 s are portrayed, alongside an all out consonant bending (THD) of 2.76%.

The outcomes demonstrate the way that the AFD can distinguish islanding with a quick identification season of under 0.06 seconds and a negligible NDZ. Islanding location depends vigorously on aggravation infusion to meet the PV network availability prerequisite. The discoveries show that when the quantity of aggravations rises, the time it takes to find islanding moves too, yet so does the consonant bending [19].

- **Description on proposed scheme**

This proposed model integrates various types of burdens into the power framework organization, including DG (photovoltaic framework), matrix, and regular burdens. Figure 14 shows a schematic of a matrix associated SPV framework that incorporates PV signals estimated at PCC for voltage and current. The ability to recognize changes or aggravations is moved by the DWT-ANN module. Its work, when it identifies an islanding circumstance, is to alarm the electrical switch with the goal that the PV framework and any adjoining loads are shielded from disturbances.

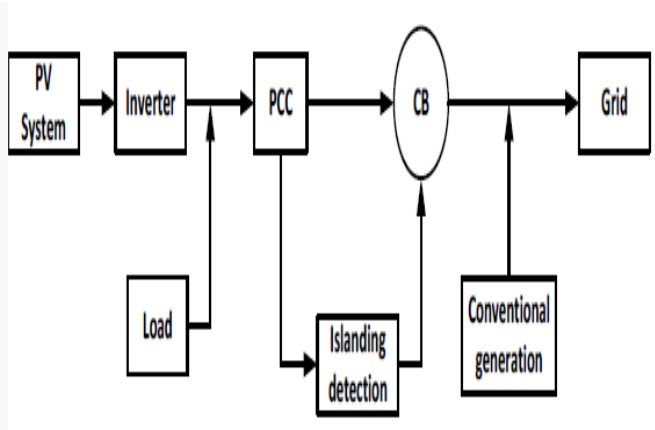

Figure 14: Grid-connected SPV system block diagram

detached recognition (VFP). Uninvolved recognition isn't absolutely practicable, as indicated by the information, because of its expansive non-identification zones. Dynamic identification technique (AFD) may reveal

islanding all the more basically and quickly, yet it corrupts power quality. These techniques have been repeated with progress utilizing Simulink, a device that accompanies MATLAB. In light of the reproduction results, it is proposed to utilize a cross breed hostile to islanding identification approach rather than a solitary location technique for better recognition proficiency. Among the upgrades are a decreased region that can't be recognized, sped up reaction times, and further developed THD power quality.

References

[1] S.Dutta, P.K.Sadhu, M.J.B.Reddy and D.K.Mohanta, "Shifting of research trends in islanding detection method-a comprehensive survey," Protection and Control of Modern Power Systems, vol. 3, no. 1, pp. 1-20, 2018.

[2] D.G.Photovoltaics and E.Storage, IEEE Standard for Interconnection and Interoperability of Distributed Energy Resources with Associated Electric Power Systems Interfaces., New York, 2018.

[3] T.Gush, S.B.A.Bukhari, R.Haider, S.Admasie, Y.S.Oh, G.J.Cho, and C.H.Kim, "Fault detection and location in a microgrid using mathematical morphology and recursive least square methods," International Journal of Electrical Power & Energy Systems, vol. 102,pp. 324-331, 2018.

[4] R.Haider, M.S.U.Zaman, S.B.A.Bukhari, Z.Ahmed, M.Mehdi, Y.S.Oh and C.H.Kim, "Protection Coordination Using Superconducting Fault Current Limiters in Microgrids," J. Korean Inst. Illum. Electr. Install. Eng, vol. 31, no. 10, pp. 26-36, 2017.

[5] A.Abokhalil, A.Awan and A.R.Al-Qawasmi, "Comparative Study of Passive and Active Islanding Detection Methods for PV Grid- Connected Systems," Sustainability, vol. 10, no. 6, p. 1798, 2018.

[6] I.Mazhari, H.Jafarian, J.H.Enslin, S.Bhowmik and B.Parkhideh, "Locking frequency band detection method for islanding protection of distribution generation," IEEE Journal of Emerging and Selected Topics in Power Electronics, vol. 5, no. 3, pp. 1386-1395, 2017.

[7] M. U. Zaman, S.Bukhari, K.Hazazi, Z.Haider, R.Haider and C.H.Kim, "Frequency response analysis of a single-area power system with a modified LFC model considering demand response and virtual inertia," Energies, vol. 11, no. 4, p. 787, 2018.

[8] T.Ghanbari, E.Farjah and F.Naseri, "Power quality improvement of radial feeders using an efficient method," Electric Power Systems Research, vol. 163, pp. 140-153, 2018.

[9] I.V.Banu, M.Istrate, D.Machidon and R.Pantelimon, "A study on antiislanding detection algorithms for grid-tied photovoltaic systems," in 2014 International Conference on Optimization of Electrical and Electronic Equipment (OPTIM) IEEE, 2014.

[10] Elshrief, Y.A., Abd-Elhaleem, S., Abozalam, B.A. and Asham, A.D., 2021. On active anti-islanding techniques: Survey. *Indonesian Journal of Electrical Engineering and Computer Science*, *17*(3), pp.1127-1134.

[11] M.Khodaparast, F. H.Vahedi and H.Oraee, "A Novel Hybrid Islanding Detection Method for Inverter-Based DGs Using SFS and ROCOF," IEEE Transactions Power Delivery, vol. 32, p. 2162–2170, 2017.

[12] S.B.A.Bukhari, R.Haider, M.S.U.Zaman, Y.S.Oh, G.J.Cho and C.H.Kim, " An interval type-2 fuzzy logic based strategy for microgrid protection," International Journal of Electrical Power & Energy Systems, vol. 98, pp. 209-218, 2018.

[13] Resende, E.C., Simoes, M.G. and Freitas, L.C.G., 2024. Anti-Islanding Techniques for Integration of Inverter-based Distributed Energy Resource to the Electric Power System. *IEEE Access*.

[14] A.Pouryekta, V.Ramachandaramurthy, S.Padmanaban, F.Blaabjerg and J.Guerrero, "Boundary Detection and Enhancement Strategy for Power System Bus Bar Stabilization—Investigation under Fault Conditions for Islanding Operation," Energies, vol. 11, no. 4, p. 889, 2018.

[15] Padmanaban, S., Priyadarshi, N., Bhaskar, M.S., Holm-Nielsen, J.B., Ramachandaramurthy, V.K. and Hossain, E., 2019. A hybrid ANFIS-ABC based MPPT controller for PV system with anti-islanding grid protection: Experimental realization. *Ieee Access*, *7*, pp.103377-103389.

[16] Hartmann, N.B., dos Santos, R.C., Grilo, A.P. and Vieira, J.C.M., 2017. Hardware implementation and real-time evaluation of an ANN-based algorithm for anti-islanding protection of distributed generators. *IEEE Transactions on Industrial Electronics*, *65*(6), pp.5051-5059.

[17] Abo-Khalil, A.G., Abdalla, M., Bansal, R.C. and Mbungu, N.T., 2023. A critical assessment of islanding detection methods of solar photovoltaic systems. *Case Studies in Thermal Engineering*, *52*, p.103681.

[18] Baghaee, H.R., Mlakić, D., Nikolovski, S. and Dragiččvić, T., 2019. Anti-islanding protection of PV-based microgrids consisting of PHEVs using SVMs. *IEEE Transactions on Smart Grid*, *11*(1), pp.483-500.

[19] Baghaee, H.R., Mlakić, D., Nikolovski, S. and Dragicević, T., 2019. Support vector machine-based islanding and grid fault detection in active distribution networks. *IEEE Journal of Emerging*

and Selected Topics in Power Electronics, *8*(3), pp.2385-2403.

[20] Nikolovski, S., Baghaee, H.R. and Mlakić, D., 2019. Islanding detection of synchronous generator-based DGs using rate of change of reactive power. *IEEE Systems Journal*, *13*(4), pp.4344-4354.

Appendix

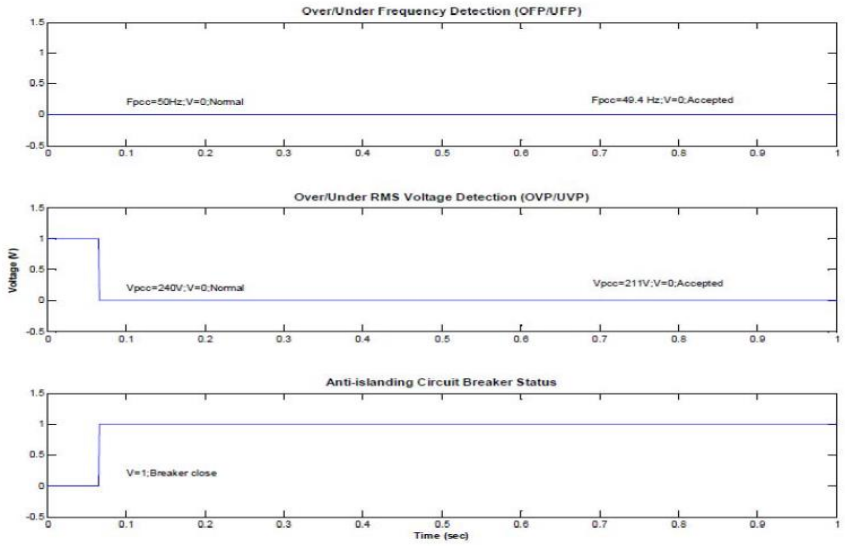

Fig.5. The detection signals for VFP under the normal operation For (a) OFP/UFP checker: V=0 (b) OVP/UVP checker: V=0 (c) Circuit breaker does not detect any abnormality.

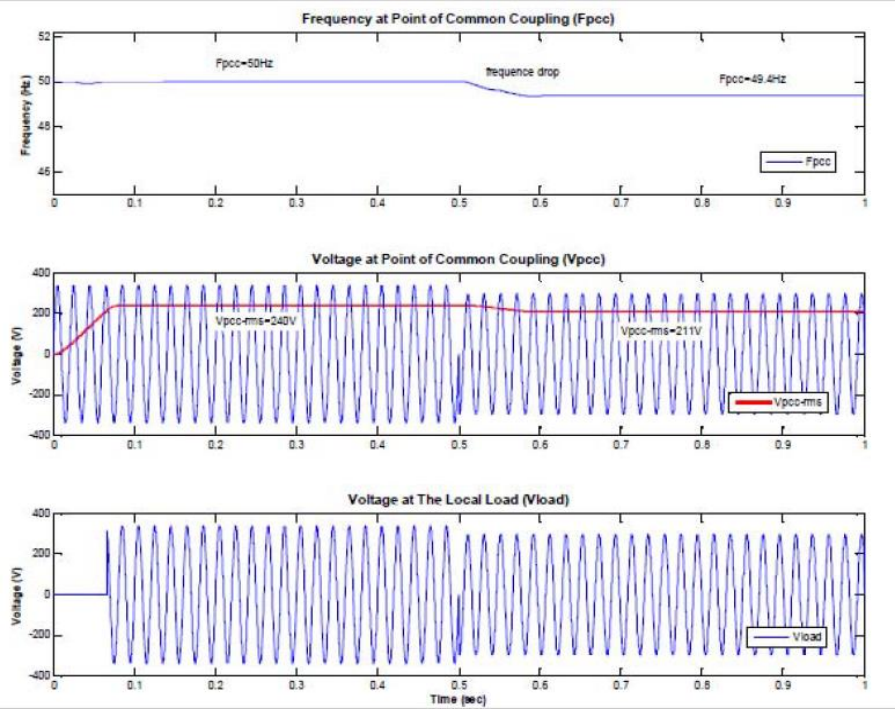

Fig.6. The simulation result for VFP at the normal operation For (a) Frequency at PCC; F_{PCC}=49.4 Hz (b) Peak–peak voltage ($V_{PCC-p.p}$) and RMS voltage at PCC: $V_{PCC-rms}$=211 V (c) Load Voltage (V_{load}): inverter continues supplying the load..

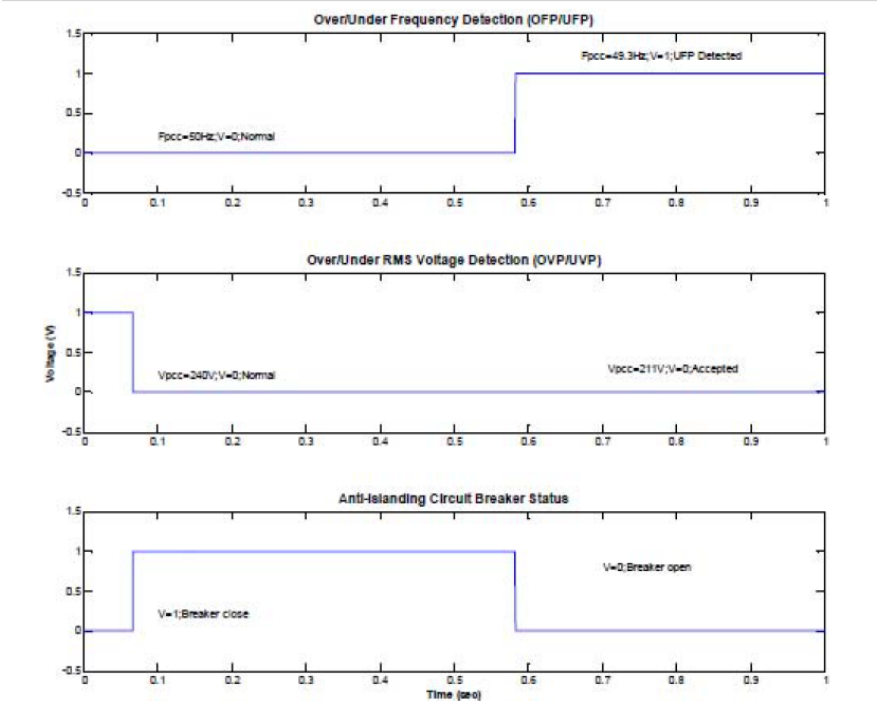

Fig.7. The detection signals for VFP under the UFP operation: for (a) OFP/UFP checker trigger UFP at t = 0.5824 s: V = 1 (b) OVP/UVP checker: V=0 (c) Circuit breaker opens at t=0.5824 s.

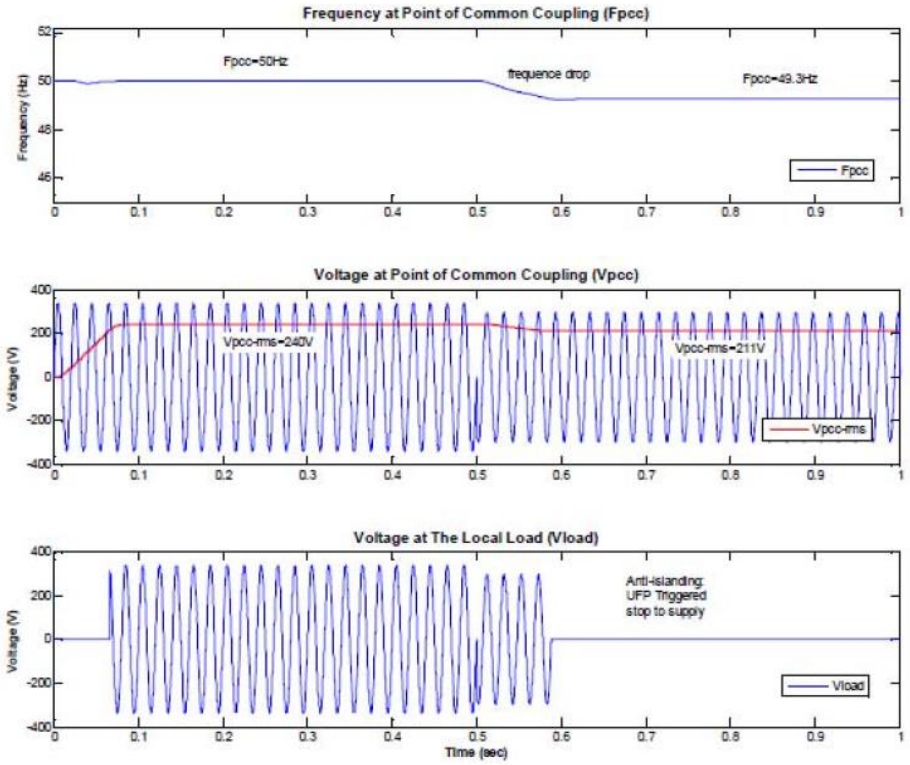

Fig.8. The simulation result for VFP under the UFP operation: for (a)F_{PCC} = 49.3 Hz (b) ($V_{PCC-p.p}$) and ($V_{PCC-rms}$) =211 V (c) Load Voltage (V_{load}): Inverter stops supplying to the load at t=0.5882 s.

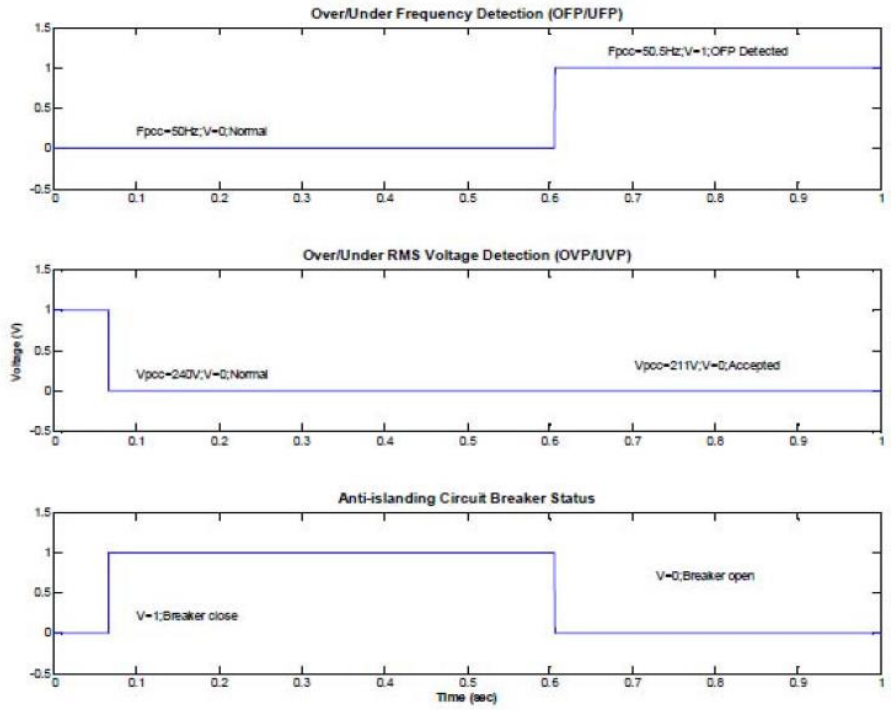

Fig.9. The detection signals for VFP under the OFP operation:V_{PCC}=211 V F_{PCC}=50.5 Hz (a) OFP/UFP checker trigger OFP at t=0.6062 s: V=1 (b) OVP/UVP checker: V=0 (c) Circuit breaker opens at t=0.6062 s.

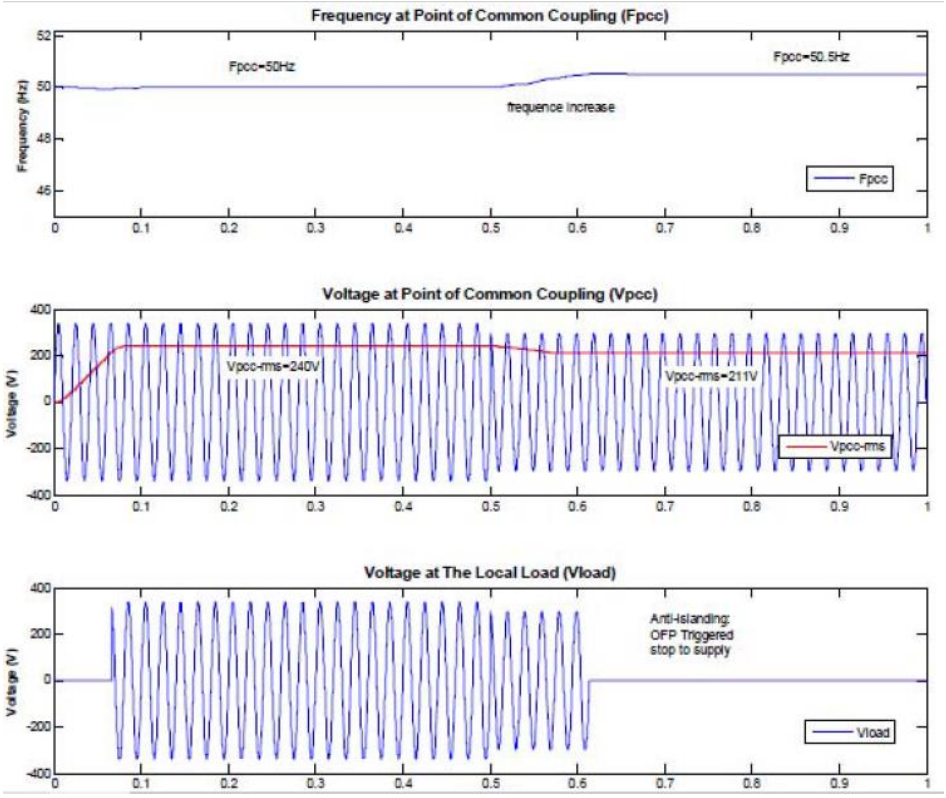

Fig.10 The simulation result for VFP under the OFP operation(a) F_{PCC}=50.5 Hz (b) ($V_{PCC-p.p}$) and $V_{PCC-rms}$=211 V (c) (V_{load}):Inverter stops supplying to the load at t=0.6140 s

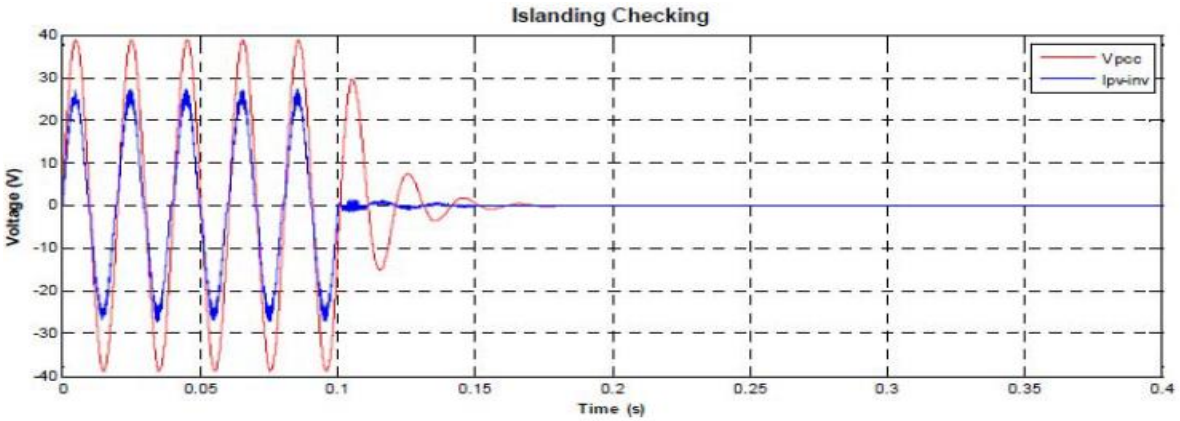

FIG.11 THE SIMULATION OUTPUT OF AFD FOR FREQUENCY=49.4 HZ, CF=0.049 Detection time, t=0.1006 s, VPCC stop at t=0.1594

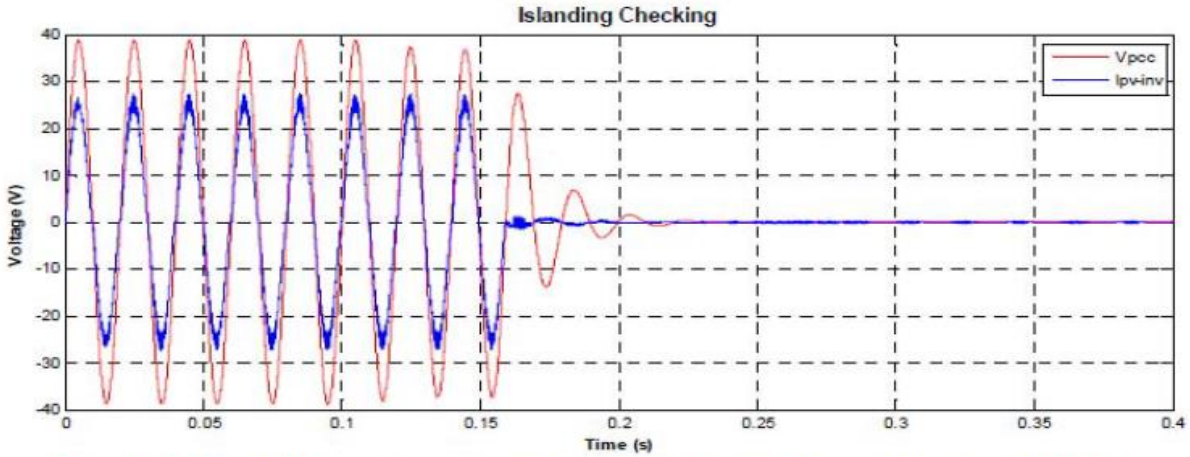

FIG.12 THE SIMULATION OUTPUT OF AFD FOR FREQUENCY=50.0 HZ, CF=0.05 Detection time, t=0.1591 s and load VPCC stop at t=0.2171 s

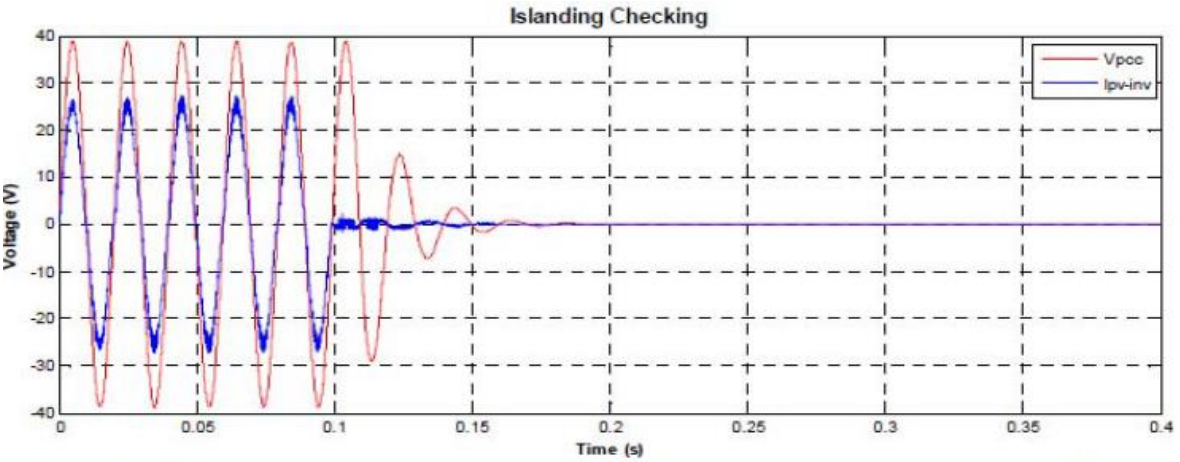

FIG.13. THE SIMULATION OUTPUT OF AFD FOR FREQUENCY=50.4 HZ, CF=0.0504 DETECTION TIME, T=0.1005 S AND LOAD VPCC STOP AT T=0.0.1672 S